Interaction of period-1 orbits in a dual-frequency driven asymmetric nonlinear oscillator

Ferenc Hegedűs*, Werner Lauterborn**, Ulrich Parlitz *** and Robert Mettin**
*Department of Hydrodynamic Systems, Budapest University of Technology and Economics, Budapest, Hungary
**Drittes Physikalisches Institut, Georg-August-Universität Göttingen, Göttingen, Germany
***Biomedical Physics Group, Max Planck Institute for Dynamics and Self-Organization, Göttingen, Germany and Institute for Nonlinear Dynamics, Georg-August-Universität Göttingen, Göttingen, Germany

Summary. The bifurcation structure of period-1 solutions of a dual-frequency driven asymmetric nonlinear oscillator (Keller–Miksis equation, describing bubble dynamics) is examined. The applied frequencies are $\omega_1/\omega_0 = 2$ and $\omega_2/\omega_0 = 3$, where ω_0 is the linear, undamped resonance frequency of the system. The control parameters were the amplitudes of the driving. Due to the specific choice of the frequency ratio and Poincaré section, the period-2 and period-3 orbits (corresponding to the monofrequency drivings of $\omega_1/\omega_0 = 2$ and $\omega_2/\omega_0 = 3$, respectively) are decomposed into a multitude of period-1 orbits. The combination of the two frequency components results in a complex bifurcation structure and interaction of these solutions in the parameter plane of the driving amplitudes.

Introduction

Dual-frequency driven nonlinear oscillators are thoroughly investigated during the last decades. From the early 80's, researchers paid special attention to quasiperiodically driven systems (using incommensurable frequencies) producing a special kind of solution called strange nonchaotic attractor [1]. It is strange due to its fractal nature but nonchaotic because it does not possess positive Lyapunov exponents. The application of a second frequency component is also successfully used for chaos control to eliminate unpredictable behaviour of certain systems [2]. Moreover, vibrational resonance induced by the application of two distant frequencies plays an important role in many experiments [3].
The bifurcation structure in the two-dimensional parameter space of the driving with fixed, commensurable frequencies, however, is less elaborated. This is the main topic of the present study. The employed Keller–Miksis equation is a second order ordinary nonlinear differential equation widely used to model the oscillation of a single spherical gas bubble in a liquid domain irradiated with high intensity ultrasound [4]. This model was successfully used to improve the efficiency of sonochemistry, material chemistry and food processing [5]. This study is to be understood as a very first research step to possible further improvement of such applications.

Mathematical model

The mathematical model describing the radial oscillation of a single spherical bubble (Keller–Miksis equation) can be written as

$$\left(1-\frac{\dot R}{c_L}\right)R\ddot R+\left(1-\frac{\dot R}{3c_L}\right)\frac{3}{2}\dot R^2=\left(1+\frac{\dot R}{c_L}+\frac{R}{c_L}\frac{d}{dt}\right)\frac{(p_L-P_\infty-p_\infty(t))}{\rho_L}, \tag{1}$$

$$p_L=p_G+p_V-\frac{2\sigma}{R}-4\mu_L\frac{\dot R}{R},\quad p_G=\left(P_\infty-p_V+\frac{2\sigma}{R_E}\right)\left(\frac{R_E}{R}\right)^{3n}, \tag{2}$$

where $R(t)$ is the time dependent bubble radius. For the details of the model see [4]. The parameter values during the computations (gas bubble in water) were as follows: liquid density $\rho_L = 997.1\,\mathrm{kg/m^3}$, sound speed $c_L = 1497.3\,\mathrm{m/s}$ and viscosity $\mu_L = 8.902^{-4}\,\mathrm{Pa\,s}$; vapour pressure $p_V = 3166.8\,\mathrm{Pa}$; surface tension $\sigma = 0.072\,\mathrm{N/m}$; ambient (static) pressure $P_\infty = 1\,\mathrm{bar}$; bubble size $R_E = 10\,\mu\,\mathrm{m}$; polytropic exponent $n = 1.4$ (adiabatic behaviour). The dual-frequency driving of the system

$$p_\infty(t) = p_{A1}\sin(\omega_1 t) + p_{A2}\sin(\omega_2 t) \tag{3}$$

is a time varying pressure field, where p_{A1} and p_{A2} are the pressure amplitudes (also control parameters); $\omega_1 = 3\omega_0$ and $\omega_2 = 2\omega_0$ are the corresponding angular frequencies. Here ω_0 is the linear undamped resonance frequency [4].
By introducing dimensionless time $\tau = t\,\omega_1/2\pi$ and bubble radius $y_1 = R/R_E$, the dimensionless bubble wall velocity y_2 and the dual-frequency driving become $y_2 = \dot R\,2\pi/(R_E\omega_1)$ and

$$p_\infty(\tau) = p_{A1}\sin(2\pi\tau) + p_{A2}\sin(2\pi\omega_2/\omega_1\tau), \tag{4}$$

respectively. Observe that the periods of the first and second components are $T_1 = 1$ and $T_2 = \omega_1/\omega_2 = 1.5$, respectively. The periodicity of the dual frequency driving is $T = 3$ (the smallest integer multiple of both T_1 and T_2), which is used for a global Poincaré map. Therefore, in the specific case of $p_{A1} = 0$ only points after every second real driving period are sampled, while in case of $p_{A2} = 0$ only after every third real driving period.

Bifurcation structure of period-1 orbits

To obtain a global picture about the co-existing attractors in the p_{A1}-p_{A2} bi-parametric plane, 10 initial value problems (IVP) were solved with random initial conditions at each parameter pair. The resolution of the pressure amplitudes were $\Delta p = 0.01\,\mathrm{bar}$ in both directions. After the initial transient, a number of 128 Poincaré points were recorded. To solve the 2.5 million IVPs within reasonable time, an in-house numerical code was used to exploit the huge computational capacity of GPUs (Nvidia Tesla K20m), with which the computational time took only $25.7\,\mathrm{h}$. The integration algorithm was the adaptive Runge–Kutta–Cash–Karp method.
The left hand side of Fig. 1 is a condensed view of the found attractors, where the colorbar represents periodicities up to period-9 (the black region is a mixture of chaotic and higher periodic solutions). The overlapping periodic domains show rich dynamics, from which only the period-1 solutions (grey area) are investigated in more details. The middle of Fig. 1 shows the number of the co-existing period-1 solutions, where the overlapping domains indicate a complex structure of period-1 attractors hidden in the grey area in Fig. 1 left which indicates only the presence of at least 1 period-1 solution.

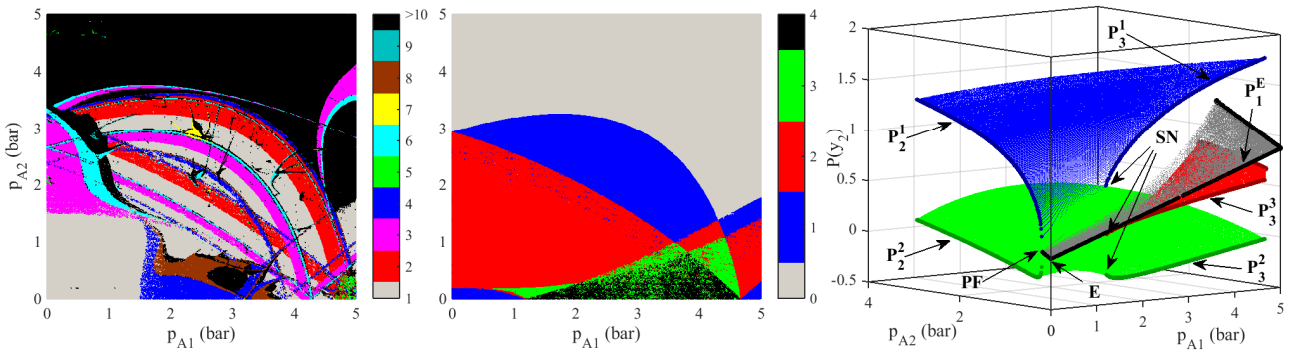

Figure 1: Left: Periodicities of the co-existing attractors. Middle: Number of the co-existing period-1 solutions. Right: Three-dimensional representation of the second component of the Poincaré section points $P(y_2)$ over the p_{A1}-p_{A2} plane.

The period-1 structure is more visible in the 3D representation of the second component of the Poincaré section points $P(y_2)$ (dimensionless bubble wall velocity) over the p_{A1}-p_{A2} plane (Fig. 1 right) where the period-1 orbits form surfaces. The solutions composing the black surface P_1^E originates from the equilibrium solution denoted by E (observe that the velocity $y_2 = 0$ at $p_{A1,2} = 0$). If $p_{A1} = 0$, an originally period-2 solution is decomposed into two period-1 solutions P_2^1 and P_2^2 emerged via a pitchfork bifurcation (PF), since $T = 2T_2$ is used for a global Poincaré section instead of T_2 itself (see the discussion in the previous section). Similarly, in case of $p_{A2} = 0$, an originally period-3 solution, appeared through a saddle-node (SN) bifurcation, splits into three period-1 solutions P_3^1, P_3^2 and P_3^3 ($T = 3T_1$). The layers of period-1 orbits marked by P_1^E and P_3^3 are "standalone" surfaces. Observe, however, that there are smooth transformations between following pairs of decomposed orbits: P_2^1-P_3^1 and P_2^2-P_3^2.

Discussion

It has been shown that the period-1 orbits form multiple surfaces in the p_{A1}-p_{A2} parameter plane. This is the consequence of the specific choice of the global Poincaré section, which decomposes the period-2 and period-3 orbits into several period-1 solutions under monofrequency driving. This is not surprising, and the difference between the decomposed solutions is only a shift in time by the corresponding monofrequency driving period. Under dual-frequency excitation, however, these solutions become distinct. Moreover, an interaction between the originally period-2 and period-3 solution can be observed via the splitting mechanism, see again Fig. 1 right. Up to our knowledge, this behaviour in dual-frequency driven system has not been observed previously.

Acknowledgement

This paper was supported by the Deutsche Forschungsgemeinschaft (DFG) grant no. ME 1645/7-1, and by the János Bolyai Research Scholarship of the Hungarian Academy of Sciences.

References

[1] Grebogi, C., Ott, E., Pelikan, S., Yorke, J. A. (1984) Strange attractors that are not chaotic. *Physica D* **13**:261-268.

[2] Behnia, S., Sojahrood, A. J., Soltanpoor, W., Jahanbakhsh, O. (2009) Suppressing chaotic oscillations of a spherical cavitation bubble through applying a periodic perturbation. *Ultrason. Sonochem.* **16**:502-511.

[3] Jeyakumari., S., Chinnathambi, V., Rajasekar, S., Sanjuan, M. A. F. (2011) Vibrational resonance in an asymmetric Duffing oscillator. *Int. J. Bifurcat. Chaos* **21**:275-286.

[4] Lauterborn, W. and Kurz, T. (2010) Physics of bubble oscillations. *Rep. Prog. Phys.* **73**:106501.

[5] Leonelli, C., Mason, T. J. (2010) Microwave and ultrasonic processing: Now a realistic option for industry. *Chem. Eng. Process.* **49**:885-900.